Formation of N719 Dye Multilayers on Dye Sensitized Solar Cell Photoelectrode Surfaces Investigated by Direct Determination of Element Concentration Depth Profiles

ARTICLE *in* LANGMUIR · MAY 2012

Impact Factor: 4.46 · DOI: 10.1021/la300077g · Source: PubMed

6 AUTHORS, INCLUDING:

Rick B Walsh
Australian National University
10 PUBLICATIONS **50** CITATIONS
SEE PROFILE

Lars Kloo
KTH Royal Institute of Technology
194 PUBLICATIONS **6,577** CITATIONS
SEE PROFILE

Jamie S Quinton
Flinders University
95 PUBLICATIONS **907** CITATIONS
SEE PROFILE

Gunther G Andersson
Flinders University
80 PUBLICATIONS **812** CITATIONS
SEE PROFILE

Langmuir

Article

pubs.acs.org/Langmuir

Formation of N719 Dye Multilayers on Dye Sensitized Solar Cell Photoelectrode Surfaces Investigated by Direct Determination of Element Concentration Depth Profiles

Lilian Ellis-Gibbings,[†] Viktor Johansson,[‡] Rick B. Walsh,[§] Lars Kloo,[‡] Jamie S. Quinton,[†] and Gunther G. Andersson*[,†]

[†]Flinders Centre for NanoScale Science and Technology, Flinders University, PO Box 2100, Adelaide SA 5001, Australia

[‡]Applied Physical Chemistry, KTH Royal Institute of Technology, S-10044 Stockholm, Sweden

[§]Department of Applied Mathematics, Research School of Physics and Engineering, The Australian National University, Canberra ACT 0200 Australia

Supporting Information

ABSTRACT: The structure of the dye layer adsorbed on the titania substrate in a dye-sensitized solar cell is of fundamental importance for the function of the cell, since it strongly influences the injection of photoelectrons from the excited dye molecules into the titania substrate. The adsorption isotherms of the N719 ruthenium-based dye were determined both with a direct method using the depth profiling technique neutral impact collision ion scattering spectroscopy (NICISS) and with the standard indirect solution depletion method. It is found that the dye layer adsorbed on the titania surface is laterally inhomogeneous in thickness and there is a growth mechanism already from low coverage levels involving a combination of monolayers and multilayers. It is also found that the amount of N719 adsorbed on the substrate depends on the titania structure. The present results show that dye molecules in dye-sensitized solar cells are not necessarily, as presumed, adsorbed as a self-assembled monolayer on the substrate.

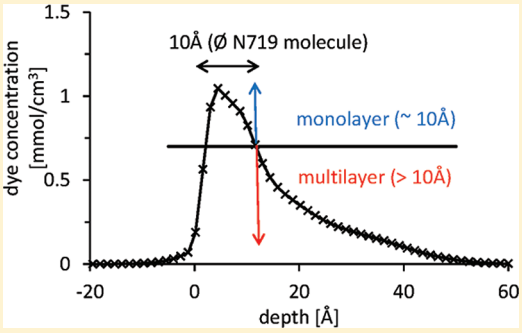

INTRODUCTION

Our society relies on electricity and energy in various forms: in 2008, the total world energy consumption was approximately 12 billion tonnes of oil equivalent.[1] Sustainable production of energy is considered to be one of the top ten challenges to mankind over the coming decade.[2] Fossil fuels constitute about 68% of the total global energy consumption.[1] However, the volumes of fossil fuels extracted per annum is expected to peak within the next few years[2] or the next few decades.[1] In order to keep energy production sustainable and cost-efficient for future generations, research must be undertaken regarding renewable energy sources. In this perspective, new-generation photovoltaic solar cells, such as the dye-sensitized solar cells (DSCs), offer one promising alternative.

One major advantage of DSCs is the expected low cost of production, as compared to traditional Si solar cells,[3,4] combined with high conversion efficiencies. DSCs were significantly improved by the introduction of a nanoporous photoelectrode in 1991 by O'Regan and Grätzel.[5] The cell they described consisted of a film of nanometer-sized, sintered titanium dioxide (titania) particles as wide bandgap substrate coated with a sensitizing organometallic dye. The DSC is an electrochemical cell, thus also consisting of a counter electrode (cathode) and an electrolyte. The function of the cell can be divided into a few steps. The sensitizing dye is excited by photon absorption, after which fast electron injection into the titania takes place.[6] Anatase is experimentally verified as the preferred titania crystal form producing the most efficient cells.[7] The injected photoelectrons are transported in the conduction band of the titania to the transparent conducting glass substrate. The sensitized titania film is in contact with the redox-active electrolyte. The main function of the electrolyte is to regenerate (reduce) the oxidized dye on the photoanode surface. The redox system is reduced at the counter electrode. Until very recently, the iodide/triiodide redox system has offered the best performance in DSCs. Its fast kinetics of dye regeneration and slow kinetics of unwanted recombination reactions at the photoelectrode surface give efficient cells with relatively low losses. Of the many sensitizing dyes investigated, the family of ruthenium-polypyridyl complexes anchored through carboxylic groups represent one of the most common and best-performing classes of dyes in DSCs.

The sensitizing dye molecules are attached to the titania surface through chemisorption via the anchoring groups. The exact nature of the binding is not fully clarified and involves a mixture of coordination modes.[8,9] Chemisorption is preferred

Received: January 5, 2012
Revised: May 8, 2012
Published: May 14, 2012

over physisorption, which does not mediate efficient electron transfer to the titania substrate.[10,11] Obviously, chemisorption to the surface will only occur in a monolayer, and as such, full coverage of a monolayer, the self-assembled monolayer, is considered and expected to be the most efficient dye interface configuration of a cell. Titania surfaces with full coverage are also preferable over partially covered surfaces for several reasons. Full dye coverage is expected to increase dye to dye electron transfer.[12,13] Further, a complete dye layer will reduce recombination losses by physically separating the electrolyte solution and the titania. Also, full coverage can be expected to maximize the absorption efficiency, as well as photoelectron injection efficiency.

Ever since the early days of DSC research, it has been presumed that the dye molecules self-assemble into an essentially perfect monolayer on the titania surface.[4,9,14−20] The assumption of the monolayer formation is based on adsorption isotherms[15,21−26] obtained from indirect methods. The total adsorption as a macroscopic quantity is typically recorded and then fitted to a model providing a molecular understanding of the origin of the data. This approach allows only for indirect conclusions. A more accurate way for determining whether dye monolayers or multilayers are formed is by employing direct methods. However, there are few experimental techniques that offer direct information about the interface structure and the dye organization. Even photoelectron spectroscopy, often regarded as a direct interface technique, only allows the determination of whether or not coverage of the titania surface by dye molecules is saturated.[27] It should thus be noted that investigations based on direct methods supporting the presumption of self-assembled dye monolayers in DSCs are lacking. Instead, the pronounced dye−dye interaction causing aggregation is a reason for concern. Is the dye−surface interaction strong enough to minimize the inherent tendency of the dye molecules to aggregate? Dye aggregation must affect photoelectron injection efficiency and thereby the overall conversion efficiency. A recent atomic force microscopic (AFM) study emphasizes this concern.[28] It is thus of central importance to understand the dye molecule adsorption characteristics in order to optimize the dye layer formation. In some cases, indirect hints have been found that dye multilayers could form in DSCs.[22,29]

The adsorption of molecules is traditionally studied using the classical method of solution depletion, whereby a known surface area is exposed to a solution of adsorbate and the concentration of the solution is determined before and after adsorption. This has recently been employed for the commonly employed sensitizing dye N719 on particulate titania.[28] Another method often used is the desorption of the dye molecules from the sample surface.[15,16,22,29] In both cases, the accuracy of the method suffers from the fact that the electrode material used for DSCs is porous and the total surface area of the electrode has to be estimated.

For a more accurate investigation of the adsorption in these systems, experiments must be performed on a sintered titania surface similar to those used in DSCs. Neutral impact collision ion scattering spectroscopy (NICISS) is an experimental technique for the determination of the depth profile of elements near the surface up to a depth of a few tens of nanometres. In contrast to the solution depletion technique, NICISS is a direct technique with the potential to give more accurate information at, in particular, lower surface coverage.

Using the NICISS technique, the average amount of an element present on a surface can be determined, as well as the average thickness and homogeneity of the adsorbed thin layer. The technique can readily be applied to systems with surfaces that are not perfectly flat. This technique has previously been used to study both solid[30] and liquid interfaces.[31] It is clear that the technique is highly suitable for the investigation of organic/inorganic interfaces.

The aim of the present work is to determine the adsorption isotherm for N719 on a mesoporous titania surface. Also, the homogeneity and the thickness of the adsorbed layer formed on the surface at various degrees of surface coverage are studied, and thus, the fundamental question of monolayer formation can be probed. The samples have been prepared using the same procedure as in the fabrication of DSCs. The isotherms obtained from direct and indirect techniques are compared and evaluated. Further, results from layers of N719 adsorbed on flat surfaces obtained from atomic layer deposition (ALD) are analyzed and compared to those from porous substrates allowing the comparison of results from both a structurally complex and simple model system.

EXPERIMENTAL SECTION

Materials and Sample Preparation. Two types of titania surfaces were used in this work. Flat titania samples were prepared via ALD on silicon wafers. Before being placed in the reaction chamber, the silicon wafer was treated with water plasma (30 W for 90 s, followed by 50 W for 30 s). The ALD process was performed using a Savannah 100 system with titanium isoproxide as the titanium source and water as the oxygen source. Nitrogen was used as a carrier gas for the precursors and the length of the precursor pulses was 0.015 s. The chamber was purged using the pure carrier gas between pulses for a period of 10 s. The flow rate of the carrier gas throughout the reaction chamber was 20 sscm throughout the process. The reaction chamber was maintained at 250 °C, while the titanium isoproxide was preheated to 80 °C and the water was kept at ambient temperature. These settings produced films that are ∼5 nm thick and are likely to consist of polycrystalline anatase.[32,33] The surface roughness of the ALD films was determined using a Digital Instruments Multimode Nanoscope III AFM. The roughness was determined to be 0.24 nm rms over an area of 1 μm^2.

The mesoporous layers of TiO_2 were prepared using the DSL 18NR-T paste from Dyesol. The paste was used as received (batch 278) containing 19.4% TiO_2 loading with particle size averaging at 20 nm. These titania nanoparticles are predominantly of anatase structure.[34] The surfaces were prepared using the doctor blade method on a clean indium tin oxide (ITO) coated glass substrate. The thickness of the layer was determined by the thickness of the tape frame used. Subsequently, the ITO/titania, substrate was heated in an oven for 30 min at 450 ± 20 °C. The temperature was increased and decreased slowly to avoid cracking of the titania layer. The paste contains organic fillers, an organic plasticizer, and terpineol as solvent. These are burnt off during the sintering process and help to control the porosity of the layer.[35]

The ITO/titania substrates were heated to 80 °C for 15 min prior to immersion into the dye solution in order to remove surface contaminants. N719 dye ($[RuL_2(NCS)_2]$: 2 TBA (L = 2,2′-bipyridyl-4,4′-dicarboxylic acid; TBA = tetra-*n*-butylammonium) solutions were made by dissolving the appropriate mass of dye in ethanol followed by consecutive dilutions. It is worth noting that in the literature both ethanol[15,16,19−21,29,36] and acetonitrile[8,17,22,24,34] are typical solvents for dyeing of titania for both ionic and nonionic dyes. The structure of the N719 dye is shown in Figure 1. The concentrations of the dye solutions were checked using a UV−vis Varian Cary 50 spectrophotometer in the wavelength region 200−800 nm. The same reference was used for all samples (pure ethanol, 99.99%). The peak at 531−533 nm was used in conjunction with the extinction coefficient 1.58×10^4

dx.doi.org/10.1021/la300077g | Langmuir 2012, 28, 9431−9439

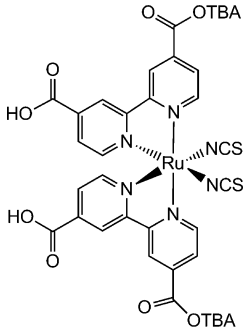

Figure 1. Structure of the N719 dye.

L mol^{-1} cm^{-1}.[37] The titania samples were dyed for 24 h in approximately 4 mL solution and rinsed thoroughly with ethanol prior to analysis. The dyed titania samples were kept in sealed containers protected from light. The typical sample size was approximately 1.5 cm^2.

The dye adsorption was investigated using NICISS for concentrations ranging from 0.0005 mmol/L to 1 mmol/L. The concentrations shown are the initial solution concentrations. For low concentrations, the concentration of the dye solution changes significantly during the adsorption process and the effect associated with this change will be discussed below (vide infra).

NICISS. The design of the NICISS equipment is described in ref 31. However, a brief summary is given here. Further experimental details can be found in the Supporting Information. NICISS is a technique for determining the concentration depth profiles of the elements at soft matter surfaces up to a depth of about 20 nm and with a resolution of a few angstroms in the near-surface area.[31] In a NICISS experiment, the target is bombarded with a pulsed beam of inert gas ions—most commonly helium ions—with a kinetic energy of several keV.[31] The energy of the projectiles backscattered from the atoms in the target is determined by their time-of-flight (TOF) from the target to the detector. The projectiles lose energy during the backscattering process, and the energy transfer depends on the mass of the target atom. This first type of energy loss is used to identify the element from which a projectile is backscattered. The projectiles also lose energy on their trajectory through the bulk due to small angle scattering and electronic excitations of the molecules constituting the target (stopping power).[38] This energy loss is used to determine the depth of the atom from which a projectile is backscattered. In combination, these two types of energy losses are used to determine the concentration depth profiles of the elements. Helium cannot be backscattered from hydrogen, as the latter is lighter than helium. Thus, no energy loss profiles of hydrogen appear in NICIS spectra, but instead, a broad background of sputtered hydrogen is present. The data evaluation to obtain the concentration depth profiles is described in detail in ref 39. NICISS has previously been used to analyze the interface structure in DSCs.[28]

Solution Depletion. The solution depletion experiments were performed in a different laboratory than the NICISS measurements. In order to determine the dye adsorption using the solution depletion method, mesoporous TiO_2 films were fabricated using a similar method as described above with the following exceptions. Films were screen-printed on fluorine-doped tin oxide (FTO) glass substrates (Pilkington TEC-8) using the same DSL 18NR-T paste from Dyesol. Screen printing typically results in somewhat more uniform TiO_2 films than doctor blading of the films. However, the influence on the dye organization due to the use of two different film-forming techniques is expected to be negligible. The titania films were submitted to the same heat treatment as described above and measured 5 × 5 mm^2 with a thickness of 10 μm.

In order to determine the concentration dependence, we prepared 37 dye solutions of N719 using 99.7% ethanol as solvent with concentrations ranging from 0.003 mmol/L to 0.200 mmol/L. The dye solutions were obtained by diluting a stock solution of known concentration in single steps. Each solution was then divided into two separate vials; into one of the sample vials, a single TiO_2/FTO substrate was immersed (3–6 mL depending on starting concentration) and the other vial was kept as reference (3 mL). All vials were stored in darkness at room temperature.

After 24 h, the TiO_2/FTO substrates were removed from the sample vials. The absorbance spectra of all solutions were recorded using a Cary 300 Bio UV–vis spectrophotometer. The amount of adsorbed dye was calculated by directly recording the difference in absorbance using the 533 nm peak comparing the sample vial solution to the reference solution for each data point. A concentration calibration curve obtained from the reference solutions was used to determine the dye concentration in solution after adsorption.

RESULTS AND DISCUSSION

NICIS Spectra. NICIS spectra of the dye N719 adsorbed on the porous and the ALD titania surfaces are shown in Figure 2.

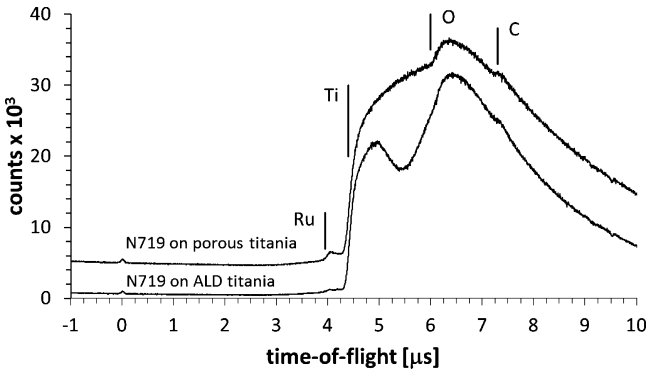

Figure 2. NICIS spectra of N719 adsorbed on a porous titania and on ALD titania substrates.

Features due to the presence of the elements carbon, oxygen, titanium, and ruthenium, i.e., the main elements constituting the samples, can be seen in the spectra. Carbon is part of the dye, oxygen is part of the dye and the substrate, titanium is part only of the substrate, and ruthenium is only part of the dye. Titanium appears as a step with only an onset in the spectrum of the dye on the porous titania substrate, since the depth in which titanium can be found in this sample is much larger than the probing depth of the NICISS technique. Titanium appears as a step with an onset and a cutoff in the spectrum of the dye on the ALD titania substrate, since the ALD titania is thinner than the probing depth of NICISS. Both ruthenium and carbon can be used to quantify the amount of substance adsorbed on both substrates and to analyze the thickness and shape of the adsorbed layer. The amount of sulfur and nitrogen in the sample is too low to cause a noticeable contribution to the spectrum, in particular, since their signal appears on top of a large background.

The contribution of each element can be separated from the total spectrum by subtracting a polynomial function fitted to the background.[39] In the present case, the background can be determined using the spectrum of the bare substrate.

The concentration depth profiles of ruthenium on the porous titania and the ALD titania are shown in Figure 3. In general, from the concentration depth profiles of ruthenium the coverage of the titania with dye, as well as the thickness and homogeneity of the thickness, can be determined. However, in the present case also the shape of the surface has to be taken into account in the data evaluation, since the porous titania substrate consists of nanoparticles. Obviously, such a surface is not flat. Helium ions will travel a longer path length through

dx.doi.org/10.1021/la300077g | Langmuir 2012, 28, 9431–9439

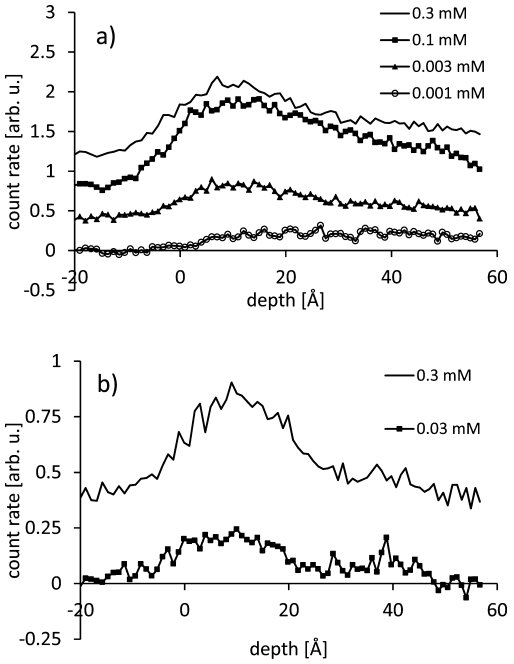

Figure 3. Measured concentration depth profiles of ruthenium of the N719 dye on (a) porous titania substrates for 0.3, 0.1, 0.003, and 0.001 mM and 0.001 mM N719 solutions and (b) on ALD titania substrates for 0.3 and 0.03 mM N719 solutions. The profiles are vertically offset for clarity.

the dye layer than the actual thickness of this layer when impacting the surface at any point that is not the center of a particle (see Figure 4). Consequently, the spectra will show

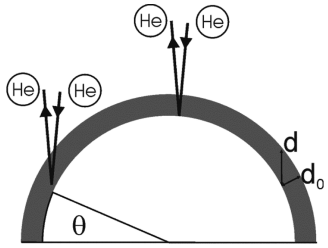

Figure 4. Schematic illustrating the relation between the length of the trajectory and the depth for a single titania nanoparticle. The image represents a view from the side. The correlation between the length of the trajectory d and the depth d_0 is illustrated.

ruthenium (the indicator element for the N719 dye) at a depth greater than the thickness of the dye layer. The concentration depth profile of the layer formed by the dye molecules on the titania nanoparticles can be derived by relating the length of the projectile trajectory to the depth in the dye layer, which is illustrated in Figure 4.

Influence of the Shape of the Surface on the NICIS Spectra. In order to separate the concentration depth profiles from the influence of the energy resolution and the shape of the surface on the spectra, a fitting procedure is applied. The fitting procedure consists of two steps. First, the concentration depth profiles are deconvoluted for the energy resolution of the method as described above. Second, the shape of the surface, i.e., the spherical nature of the titania particles, is taken into account. The second procedure is described in the Supporting Information.

Figure 5 illustrates the interpretation of the shape of the concentration depth profile after applying the second step of

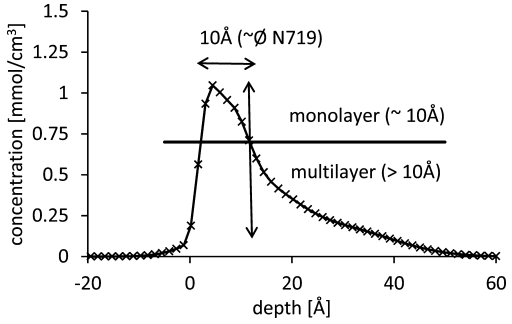

Figure 5. Concentration depth profile of the sample immersed into the 0.3 mM N719 dye solution. The measured profile is deconvoluted and corrected for the spherical nature of the substrate (the procedure taking the spherical nature of the substrate into account is described in the Supporting Information). The profile shows that a fraction of the surface is covered with a monolayer of the dye (region with a thickness <10 Å, fraction indicated with the upper arrow) and a region with multilayers (region with a thickness >10 Å, fraction indicated with the lower arrow). The choice of 10 Å for separating mono- and multilayer is to some degree arbitrary.

the fitting procedure. The profile shows that a fraction of the surface is covered with a monolayer of the dye (region with a thickness <10 Å, i.e., a monolayer of dye would result in a concentration depth profile with a thickness of <10 Å) and a region with multilayers (region with a thickness >10 Å, i.e., a multilayer of dye would result in a concentration depth profile with a thickness of >10 Å). For the separation into mono- and multilayers, a thickness of 10 Å was chosen on the basis of the approximate size of a N719 molecule.[40]

In Figure 6a, the concentration depth profiles of porous titania substrates immersed into dye solutions are shown. All four profiles are deconvoluted and corrected for the spherical nature of the porous titania substrate. In Figure 6b, the deconvoluted concentration depth profiles of ruthenium of the ALD titania immersed into 0.3 and 0.03 mM N719 dye are shown. The details of these figures will be discussed later.

Adsorption Isotherm and Growth of the Dye Layer. In Figure 7, the amount of dye adsorbed on the titania for both the porous and the ALD titania surfaces is shown as a function of the N719 concentration. The amount of dye adsorbed on the titania surface is determined by integrating each concentration depth profile. In the case of the porous titania substrate, the profile corrected for the influence of the shape of the spheres is integrated. The coverage is given in the amount of dye per surface area. The surface area in the case of the nanoporous titania is the surface area of the nanoparticles and not the macroscopic size of the sample. It can be seen that the coverage of the titania increases monotonously with the concentration of the dye solution and levels off at higher concentrations. It has to be noted that the concentration shown on the abscissa in Figure 7 is the initial concentration of the dye solution. As described in the sample preparation, the total amount of the dye solutions was kept at about 4 mL. The total amount of dye in the solution will change significantly during the adsorption process and thus also the concentration of the solution. Hence, the concentration given on the abscissa of Figure 7 for the graph of the porous titania substrate is not the equilibrium concentration. In the case of the ALD titania, the concentration

dx.doi.org/10.1021/la300077g | Langmuir 2012, 28, 9431−9439

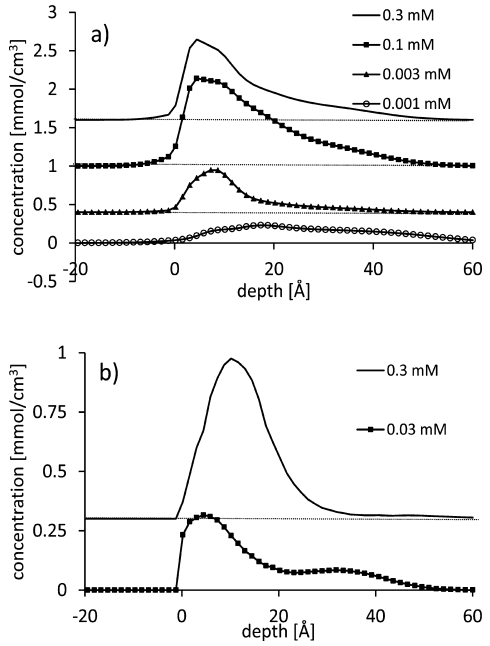

Figure 6. Concentration depth profiles of the ruthenium of the N719 dye adsorbed on (a) porous titania surfaces for the concentrations 0.3, 0.1, 0.003, and 0.001 mM, and (b) on ALD titania surfaces for the concentrations 0.3 and 0.03 mM. The profiles are vertically offset for clarity.

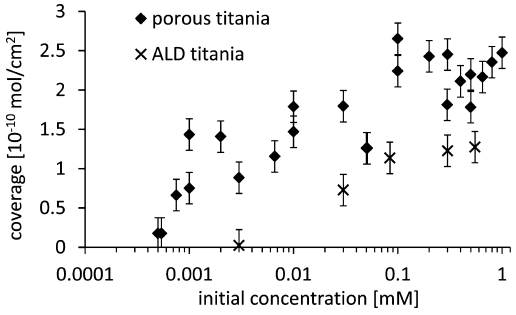

Figure 7. Adsorption isotherm of N719 on porous titania substrate and the ALD substrate as determined by the NICISS technique.

of the dye solution is not significantly reduced upon adsorption, since the total titania surface area is much smaller due to the nonporous nature of the substrate.

The adsorption isotherms on the porous titania and the ALD titania substrates determined from the ruthenium concentration depth profiles are similar in shape but differ significantly at which concentration half of the maximum concentration is reached. Furthermore, the substrates differ in their maximum coverage. In the case of the porous substrate, half of the maximum coverage is reached between a concentration of 0.002 and 0.008 mM of the dye solution. In contrast, 0.02 to 0.08 mM are required when using the ALD substrates. The difference in solution concentration at half of the maximum coverage for the two different substrates is even larger, since the equilibrium concentration of the dye solution in the case of the porous titania substrate is lower than the plotted initial dye concentration. The maximum coverage on the porous substrate calculated from the measurements with an initial dye concentration equal or greater than 0.1 mM is $(2.2 \pm 0.3) \times 10^{-10}$ mol/cm^2 (1.3 ± 0.2 molecules/nm^2) and that of the ALD titania $(1.2 \pm 0.1) \times 10^{-10}$ mol/cm^2 (0.73 ± 0.05 molecules/nm^2) (Table 1). The maximum coverage found for the case of the porous titania substrate in this study is larger than the

Table 1. Maximum Coverage and Concentration for Half Coverage for the Porous and ALD Titania Substrate

	porous titania	ALD titania
maximum coverage [10^{-10} mol/cm^2]	2.2 ± 0.3	1.2 ± 0.1
maximum coverage [molecules/nm^2]	1.3 ± 0.2	0.73 ± 0.05
concentration at half coverage [mM]	0.002−0.008	0.02−0.08

values assumed in the literature for dyes with a similar structure to that of N719. Literature values range from 0.56[36] to 1.1 molecules/nm^2.[41]

The difference in coverage of the porous titania and the ALD titania substrates can most likely be explained by the difference in surface structure. Both titania materials have a similar crystal structure. However, the nanoporous morphology is based on nanoparticles with an approximate spherical shape, while the ALD process results in an essentially flat surface. As a consequence, the number of defect sites on the nanoporous surface is expected to be much larger than on the ALD surface. It is well-known that defect sites are preferred adsorption sites, since their surface energy, as a result of coordination unsaturation, is larger than that of a perfect crystal structure.[42] Since the adsorption process is driven by a reduction in surface energy, a surface with a higher number of defect sites should allow the adsorption of a larger number of molecules as compared to a surface with a lower number of defect sites. It must be noted that from the current work, however, no evidence can be given regarding whether or not the difference in adsorption is related to differences in the density of defects on the titania surfaces.

The shape of the concentration depth profiles gives information about whether the dye molecules adsorb as mono- or multilayers. Since each dye molecule contains only one ruthenium atom, a layer in the ruthenium profiles with a thickness considerably larger than that expected of a monolayer has to be considered as a N719 multilayer. Figure 6a shows that the 0.3, 0.1, 0.003, and 0.001 mM profiles on the porous titania all have a mixture of monolayer and multilayer coverage. The ratio between the surface covered by a monolayer and the surface covered by a multilayer is about 1:2 in all cases except for the 0.001 mM solution. The 0.3 and 0.03 mM profiles on the ALD titania shown in Figure 6b have a similar ratio of monolayer and multilayer coverage as those of the porous titania substrates.

The 0.001 mM profile in Figure 6a shows only a multilayer contribution. The same was found for all six solutions with a concentration $\leq$0.002 mM. It is worth noting that the adsorption isotherm shows a reproducible minimum at slightly higher concentrations between 0.003 and 0.007 mM. Thus, the minimum in the adsorption isotherm and the change in the structure of the dye layer are correlated. It may be speculated that the adsorption mechanism for the very low concentrations is different from that at higher concentrations. At very low concentrations, only islands with a thickness of a few monolayers are formed, while a higher concentration leads to a combination of multi- and monolayers. The reason may be attributed to the defect structure of the titania surface. In the case of the ALD titania substrate, i.e., the titania substrate with the most likely lower surface density of defects, the shape of the ruthenium concentration depth profile, and thus the dye layer

dx.doi.org/10.1021/la300077g | Langmuir 2012, 28, 9431−9439

structure, does not depend on the concentration of the dye solution. Non-monotonous adsorption isotherms have been found before for the adsorption of silanes on metal oxide surfaces.[43,44]

The similarity of the shape of the concentration depth profiles found at concentrations ≥0.007 mM on the porous titania and the ALD titania substrates allows for conclusions in regard to the growth process of the dye layer. The fact that the general shape of the concentration depth profiles does not change with the total amount of adsorbed dye, i.e., with the concentration of the dye solution, and that the profiles have to be described as a combination of monolayer and multilayer coverage can only be explained with a growth mechanism of the dye layer localized at specific sites rather than a distributed growth of a layer with a uniform thickness. At each growth site, the layer thickness increases to the finite thickness. The total layer then grows by increasing the number of growth sites rather than through a simultaneous increase at each individual growth site. The growth mechanism is schematically illustrated in Figure 8. The growth mechanism for the very low

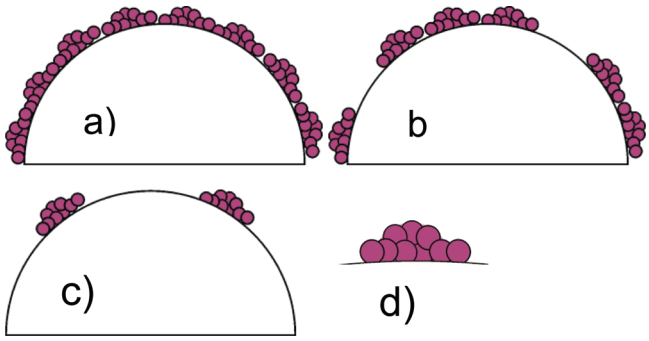

Figure 8. Schematic illustration of the proposed growth mechanism of the dye layer at specific sites with an increase of the dye coverage as increasing number of sites covered with dye: (a) maximum coverage, (b) medium coverage, (c) low coverage, and (d) structure of an individual site. Each colored circle corresponds to a single dye molecule.

concentrations might be different from the illustrated mechanism. However, since this is so far speculative, the potentially different mechanism is not illustrated. A prevailing influence of the pores of the nanoporous titania on the formation of multilayers can be excluded, since the ALD titania shows the same agglomeration of dye molecules. Furthermore, it can be noted that, if pore congestion arising from dye adsorption and potential dye aggregation were a large problem, the new types of redox systems based on transition metal complexes, such as trisbipridyl cobalt (II,III) complexes, could not work as efficient redox systems; albeit, overall efficiencies in such systems benefit from a more porous morphology.[45]

The choice of ethanol as solvent might influence the multilayer formation found here. As noted in the Experimental section, both ethanol and acetonitrile are frequently used as solvents, ethanol being the less polar solvent. It could be argued that the N719 dye agglomerates in ethanol solutions and using acetonitrile might not result in multilayer formation. It is worth considering the publication of Bazzan et al.[14] in this context. The authors have developed a method of repeated cycles of adsorption and desorption of N719. Taking the differences in porosity of the titania substrates used into account, the authors found small quantitative but no qualitative differences in the amount of dye adsorbed—as determined by UV−vis absorption spectrophotometry—as well as in the performance of the DSCs. It may thus be assumed that the formation of multilayers is not caused by the agglomeration of the dye in the solution. Further arguments in favor of this assumption can be based on the fact that in the present publication agglomeration is found at all dye concentrations, thus even at the very low concentration of 0.001 mM. At such low concentration, no significant aggregation in ethanol solution can be expected. Hence, we conclude that the formation of multilayers is not caused by the solvent chosen but instead by the nature of the adsorption process and the properties of both the substrate and the dye.

Carbon Concentration Depth Profiles. The same procedure for determining the concentration depth profiles of ruthenium can also be applied to the concentration depth profiles of carbon. The coverage of the titania with carbon is shown in Figure 9. It must be noted that the coverage is given in moles of carbon per cm^2 of the titania.

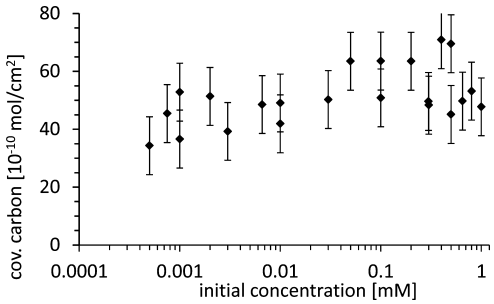

Figure 9. Coverage of the nanoporous titania with carbon. It must be noted that the coverage is given in moles of carbon per cm^2 of the titania surface. The ratio between ruthenium and the carbon in case of the ruthenium complex alone is 1:25, while the ratio between ruthenium and carbon is 1:58 in case of the entire N719 dye molecule, i.e., including the TBA.

Figure 9 shows that the coverage with carbon is almost independent of the dye concentration. Moreover, even at low concentrations of the dye solution and with very little coverage of dye, as indicated by the ruthenium signal, almost the same coverage with carbon can be found as at high concentrations of the dye solution. The ratio in the spectra between ruthenium and carbon at higher concentrations of the dye solution is 1:25 (±5). This ratio is different from the ratio between ruthenium and carbon in the N719 dye molecule, which is 1:58. This could be a hint that the amount of the cation TBP adsorbing on the titania is lower than that of the ruthenium complex. However, it has to be noted that the carbon signal is in a region of the NICIS spectrum with a large contribution of helium projectiles backscattered from titanium. Separating the carbon signal from the titanium signal is difficult, since it is unclear where the carbon contribution ends in the NICIS spectrum. In particular, it is very difficult to determine the carbon contribution with high precision at larger depth, and thus lower concentration, as the carbon step decreases gradually. Thus, the C/Ru ratio of 1:25 found has a large uncertainty and thus no further conclusions will be drawn from the ratio found.

However, the fact that the carbon signal is almost independent of the concentration of the dye solution has to be considered as significant, since the procedure to separate the carbon signal from the titanium signal has been the same for all

dx.doi.org/10.1021/la300077g | Langmuir 2012, 28, 9431−9439

spectra and the uncertainty in determining the carbon contribution at larger depth affects all spectra in the same way. The only possible explanation for this fact is that not all carbon originates from the adsorbed dye. Adventitious hydrocarbon molecules adsorbing during the substrate preparation, and possibly also solvent molecules, are most likely to cover the titania surface in addition to the dye molecules at low dye coverage; an effect also observed by Lee et al.[46] With increasing concentration of the dye solution, the dye molecules replace the adsorbed hydrocarbons. Such replacement is favorable, since the chemisorbed dye molecules binds more strongly to the surface than adventitious hydrocarbons. In this context, it can also be noted that no visual indications of dye decomposition could be observed.

Solution Depletion Method and Comparison with Adsorption Isotherm Determined by NICISS. The adsorption isotherm determined with the solution depletion method is shown in Figure 10. The graph shows the adsorbance

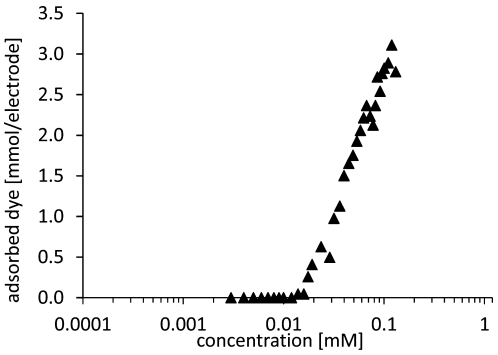

Figure 10. Adsorption isotherm of N719 on porous titania substrates determined from the solution depletion method.

of the dye on the titania from about 0.01 mM, reaches half coverage at 0.4 mM and its maximum at a concentration of about 0.1 mM. The adsorption isotherm shown here has similarities to that published by Lim et al.[24] Half coverage and maximum coverage are both reached at similar concentrations.

The solution depletion adsorption isotherm differs significantly from that determined with NICISS. The former shows an onset at more than 1 order of magnitude higher concentration as compared to the latter. The maximum, however, is reached at a similar concentration in both cases. The difference between the isotherms has most likely to be attributed to the fact that the solution depletion method becomes the more inaccurate the lower the dye concentration; i.e., the sensitivity of the UV−vis technique to changes in the dye concentration is too low at low concentrations. The UV−vis spectra at low concentrations are dominated by the features of the solvent, and consequently, small changes in the absorption at low dye concentrations are almost impossible to detect leading to a systematic error difficult to quantify. Inhomogeneous distribution of the dye throughout the titania layer due to the limitation of the diffusion of the dye molecules into the titania layer during immersion into the dye solution could be another reason for the detection of a lower adsorption of dye molecules using the solution depletion adsorption method as compared to the NICISS method.[47,48] The NICISS technique probes only the outermost layer of the samples, while the solution depletion method measures the adsorption in the entire titania layer. However, it was found that diffusion limitation plays a role only in case the titania layer was immersed for much shorter times into the dye solution than in the present case. Thus, we exclude that diffusion limitation is the reason for the differences in the adsorption isotherms. Decomposition of the dye molecules potentially could influence the depletion adsorption isotherm measurements as well in case a product of the decomposition would be detected at a similar wavelength as the dye molecule itself. However, so far we do not have any indication that this might be the case. NICISS has to be considered as the more accurate method, since it is a direct method for determining the amount of adsorbed dye. The uncertainty of the NICISS technique with respect to the amount of dye adsorbed onto the titania is shown as error bars in Figure 7. The systematic error of the solution depletion method is not known but is certainly much higher than for the NICISS method.

Despite the difference in the adsorption isotherms determined with the solution depletion method and desorption method on the one side and with NICISS on the other, there are a few similarities. In all cases, the isotherms are leveling off at higher concentrations and the overall shape bears similarities to a Langmuir adsorption isotherm. Using NICISS, we find that adsorption is in multilayers and not in monolayers, which seems to be in disagreement with a Langmuir-type adsorption isotherm. This disagreement could be resolved by considering what units are adsorbing on the titania surface. As described above, the NICISS measurements show that throughout the entire concentration range the N719 layer grows by increasing the number of growth sites rather than through a simultaneous increase at each individual growth site, where coverage in multilayers is observed at each site. In case the amount of dye adsorbing at each adsorption site is considered as a single unit, the growth mechanism could be considered as Langmuir-type adsorption by filling the maximum number of available adsorption sites. The new concept in this work is then that, at a single adsorption site, i.e., a single unit of the adsorption layer (as schematically shown in Figure 8d), the adsorbed molecules do not strictly form a monolayer but instead a multilayer structure.

■ CONCLUSIONS

The adsorption isotherm determined with NICISS shows a maximum coverage of $(2.2 \pm 0.3) \times 10^{-10}$ mol/cm^2 on the porous titania substrate and $(1.2 \pm 0.1) \times 10^{-10}$ mol/cm^2 on the ALD titania substrate. The maximum coverage is larger than estimated in the literature. Half-coverage is reached at 0.002 and 0.008 mM for the porous substrate and between 0.02 to 0.08 mM for the ALD substrate. These concentrations are not the equilibrium but the initial concentrations of the dye solutions. It is assumed that the difference between the substrates in total coverage can be explained by the difference in number of defect sites, which are usually the preferred sites for adsorption and have a higher density on the surface of the nanoporous substrate.

The adsorption isotherms determined with the solution depletion method has an onset at a much higher dye concentration as compared to the adsorption isotherm determined with NICISS. The reason for the difference is attributed to the insensitivity of the indirect, spectrophotometric technique at low concentrations.

The growth mechanism of the N719 dye layer is based on individual sites with a combination of monolayer and multilayer coverage. The growth of the fully covering layer takes place

dx.doi.org/10.1021/la300077g | Langmuir 2012, 28, 9431−9439

through an increase in the number of covered adsorption sites, rather than through a global monolayer formation. The structure and the growth mechanism are similar on the porous and the ALD substrates, and thus, the latter can be considered for model studies of the adsorption of large organic molecules on titania. The main and more general conclusion is that it cannot be taken for granted that sensitizing dyes in general form monolayers on the titania substrates in DSCs. Dye loading measurements used to estimate surface areas must therefore be taken with some reservation. In the case of multilayer formation, a large part of adsorbed dye molecules are not in direct contact with the titania surface, and photoelectron injection must be less efficient, or at least retarded. The consequence of this conclusion is that the models proposed for photoelectron injection must be questioned, and that dye molecule engineering to reduce the level of dye aggregation may prove fruitful in terms of enhanced injection efficiency or shorter injection times and ultimately higher DSC conversion efficiency.

Today, in attempts to speed up the dyeing process, such as in industrialization processes where this step may represent a bottleneck in the assembly of DSCs, preferably much higher dye concentrations are used. However, such strategies have always raised concerns regarding dye aggregation and non-efficient multilayer formation. In light of the present results, the use of higher dye concentrations in the dyeing baths may not be as detrimental as previously assumed.

■ ASSOCIATED CONTENT

Supporting Information

A detailed description of NICISS technique and the deconvolution procedure. This material is available free of charge via the Internet at http://pubs.acs.org.

■ AUTHOR INFORMATION

Corresponding Author

*E-mail: gunther.andersson@flinders.edu.au.

Notes

The authors declare no competing financial interest.

■ ACKNOWLEDGMENTS

We want to thank Flinders University for financial support, as well as the Swedish Energy Agency and the Swedish Research Council.

■ REFERENCES

(1) *World Energy Outlook 2010, Executive Summary*; International Energy Agency: Paris, 2010.

(2) Smalley, R. E. Future global energy prosperity: the terawatt challenge. *MRS Bull.* **2005**, *30* (6), 412.

(3) Grätzel, M. Photovoltaic performance and long-term stability of dye-sensitized mesosocopic solar cells. *C. R. Chim.* **2006**, *9* (5−6), 578−583.

(4) Grätzel, M. Dye-sensitized solar cells. *J. Photochem. Photobiol. C: Photochem. Rev.* **2003**, *4* (2), 145−153.

(5) O'Regan, B.; Gratzel, M. A low-cost, high-efficiency solar cell based on dye-sensitized colloidal TiO_2 films. *Nature* **1991**, *353* (6346), 737−740.

(6) Benkö, G.; Kallioinen, J.; Korppi-Tommola, J. E. I.; Yartsev, A. P.; Sundström, V. Photoinduced Ultrafast Dye-to-Semiconductor Electron Injection from Nonthermalized and Thermalized Donor States. *J. Am. Chem. Soc.* **2001**, *124* (3), 489−493.

(7) Park, N. G.; van de Lagemaat, J.; Frank, A. J. Comparison of Dye-Sensitized Rutile- and Anatase-Based TiO2 Solar Cells. *J. Phys. Chem. B* **2000**, *104* (38), 8989−8994.

(8) Nazeeruddin, M. K.; Humphry-Baker, R.; Liska, P.; Grätzel, M. Investigation of Sensitizer Adsorption and the Influence of Protons on Current and Voltage of a Dye-Sensitized Nanocrystalline TiO2 Solar Cell. *J. Phys. Chem. B* **2003**, *107* (34), 8981−8987.

(9) De Angelis, F.; Fantacci, S.; Selloni, A.; Nazeeruddin, M. K.; Grätzel, M. First-Principles Modeling of the Adsorption Geometry and Electronic Structure of Ru(II) Dyes on Extended TiO2 Substrates for Dye-Sensitized Solar Cell Applications. *J. Phys. Chem. C* **2010**, *114* (13), 6054−6061.

(10) Duffy, N. In situ infrared spectroscopic analysis of the adsorption of ruthenium(II) bipyridyl dicarboxylic acid photo-sensitizers to TiO2 in aqueous solutions. *Chem. Phys. Lett.* **1997**, *266* (5,6), 451.

(11) Hirose, F.; Kuribayashi, K.; Shikaku, M.; Narita, Y.; Takahashi, Y.; Kimura, Y.; Niwano, M. Adsorption Density Control of N719 on TiO[sub 2] Electrodes for Highly Efficient Dye-Sensitized Solar Cells. *J. Electrochem. Soc.* **2009**, *156* (9), B987−B990.

(12) Hardin, B. E.; Snaith, H. J.; McGehee, M. D. The renaissance of dye-sensitized solar cells. *Nat. Photon* **2012**, *6* (3), 162−169.

(13) Unger, E. L.; Morandeira, A.; Persson, M.; Zietz, B.; Ripaud, E.; Leriche, P.; Roncali, J.; Hagfeldt, A.; Boschloo, G. Contribution from a hole-conducting dye to the photocurrent in solid-state dye-sensitized solar cells. *Phys. Chem. Chem. Phys.* **2011**, *13* (45), 20172−20177.

(14) Bazzan, G.; Deneault, J. R.; Kang, T.-S.; Taylor, B. E.; Durstock, M. F. Nanoparticle/Dye Interface Optimization in Dye-Sensitized Solar Cells. *Adv. Funct. Mater.* **2011**, *21* (17), 3268−3274.

(15) Hwang, K.-J.; Shim, W.-G.; Jung, S.-H.; Yoo, S.-J.; Lee, J.-W. Analysis of adsorption properties of N719 dye molecules on nanoporous TiO2 surface for dye-sensitized solar cell. *Appl. Surf. Sci.* **2010**, *256* (17), 5428−5433.

(16) Katoh, R.; Yaguchi, K.; Furube, A. Effect of dye concentration on electron injection efficiency in nanocrystalline TiO2 films sensitized with N719 dye. *Chem. Phys. Lett.* **2011**, *511* (4−6), 336−339.

(17) Lee, K.-M.; Suryanarayanan, V.; Ho, K.-C.; Justin Thomas, K. R.; Lin, J. T. Effects of co-adsorbate and additive on the performance of dye-sensitized solar cells: A photophysical study. *Sol. Energy Mater. Sol. Cells* **2007**, *91* (15−16), 1426−1431.

(18) Liu, G.; Jaegermann, W.; He, J.; Sundström, V.; Sun, L. XPS and UPS Characterization of the TiO2/ZnPcGly Heterointerface: Alignment of Energy Levels. *J. Phys. Chem. B* **2002**, *106* (23), 5814−5819.

(19) Yu, Y.; Wu, K.; Wang, D. Dye-sensitized solar cells with modified TiO[sub 2] surface chemical states: The role of Ti[sup 3 +]. *Appl. Phys. Lett.* **2011**, *99* (19), 192104−3.

(20) Zhang, J.; Zaban, A. Efficiency enhancement in dye-sensitized solar cells by in situ passivation of the sensitized nanoporous electrode with Li2CO3. *Electrochim. Acta* **2008**, *53* (18), 5670−5674.

(21) Ishihara, T.; Tokue, J.; Sano, T.; Shen, Q.; Toyoda, T.; Kobayashi, N. Effect of Ligand Carboxylation on Adsorption and Photosensitization in Ru(II)-Complex Dye-Sensitized Nanocrystalline TiO2 Solar Cell. *Jpn. J. Appl. Phys.* **2005**, *44* (4B), 2780−2782.

(22) Katono, M.; Bessho, T.; Meng, S.; Humphry-Baker, R.; Rothenberger, G.; Zakeeruddin, S. M.; Kaxiras, E.; Grätzel, M. D-π-A Dye System Containing Cyano-Benzoic Acid as Anchoring Group for Dye-Sensitized Solar Cells. *Langmuir* **2011**, *27* (23), 14248−14252.

(23) Krüger, J.; Bach, U.; Grätzel, M. Modification of TiO2 Heterojunctions with Benzoic Acid Derivatives in Hybrid Molecular Solid-State Devices. *Adv. Mater.* **2000**, *12* (6), 447−451.

(24) Lim, J.; Kwon, Y. S.; Park, S.-H.; Song, I. Y.; Choi, J.; Park, T. Thermodynamic Control over the Competitive Anchoring of N719 Dye on Nanocrystalline TiO2 for Improving Photoinduced Electron Generation. *Langmuir* **2011**, *27* (23), 14647−14653.

(25) Robert, D.; Weber, J. V. Study of the Adsorption of Dicarboxylic Acids on Titanium Dioxide in Aqueous Solution. *Adsorption* **2000**, *6* (2), 175−178.

(26) Natu, G.; Huang, Z.; Ji, Z.; Wu, Y. The Effect of an Atomically Deposited Layer of Alumina on NiO in P-type Dye-Sensitized Solar Cells. *Langmuir* **2011**, *28* (1), 950−956.
(27) Yu, S.; Ahmadi, S.; Sun, C.; Palmgren, P. l.; Hennies, F.; Zuleta, M.; Göthelid, M. 4-tert-Butyl Pyridine Bond Site and Band Bending on TiO2(110). *J. Phys. Chem. C* **2010**, *114* (5), 2315−2320.
(28) Marquet, P.; Andersson, G.; Snedden, A.; Kloo, L.; Atkin, R. Molecular Scale Characterization of the Titania−Dye−Solvent Interface in Dye-Sensitized Solar Cells. *Langmuir* **2010**, *26* (12), 9612−9616.
(29) Hara, Y.; Tejedor-Tejedor, M. I.; Lara, K.; Lubin, D.; Brzozowski, L. J.; Severseike, D. J.; Anderson, M. A. Importance of adsorption isotherms in defining performance of dye-sensitized solar cells fabricated from photoelectrodes composed of ZnO nanopowders and nanorods. *Electrochim. Acta* **2011**, *56* (24), 8873−8879.
(30) Andersson, G.; Morgner, H. Determining the stopping power of low energy helium in alkanethiolates with Neutral Impact Collision Ion Scattering Spectroscopy (NICISS). *Nucl. Instrum. Methods Phys. Res., Sect. B* **1999**, *155* (4), 357−368.
(31) Andersson, G.; Morgner, H. Impact collision ion scattering spectroscopy (ICISS) and neutral impact collision ion scattering spectroscopy (NICISS) at surfaces of organic liquids. *Surf. Sci.* **1998**, *405* (1), 138−151.
(32) Heikkilä, M.; Puukilainen, E.; Ritala, M.; Leskelä, M. Effect of thickness of ALD grown TiO2 films on photoelectrocatalysis. *J. Photochem. Photobiol., A* **2009**, *204* (2−3), 200−208.
(33) Aarik, J.; Aidla, A.; Uustare, T.; Ritala, M.; Leskelä, M. Titanium isopropoxide as a precursor for atomic layer deposition: characterization of titanium dioxide growth process. *Appl. Surf. Sci.* **2000**, *161* (3−4), 385−395.
(34) Zaban, A.; Aruna, S. T.; Tirosh, S.; Gregg, B. A.; Mastai, Y. The Effect of the Preparation Condition of TiO2 Colloids on Their Surface Structures. *J. Phys. Chem. B* **2000**, *104* (17), 4130−4133.
(35) Gratzel, M.; Durrant, J. R. Dye Sensitised Mesoscopic Solar Cells. In *Nanostructured and Photoelectrochemical Systems for Solar Photon Conversion*, Archer, M. D., Nozik, A. J., Eds.; Imperial College Press: London, 2007; pp 503−536.
(36) Kavan, L.; Grätzel, M.; Gilbert, S. E.; Klemenz, C.; Scheel, H. J. Electrochemical and Photoelectrochemical Investigation of Single-Crystal Anatase. *J. Am. Chem. Soc.* **1996**, *118* (28), 6716−6723.
(37) Kong, F.; Fantai, F. Kong, Purification of bipyridyl ruthenium dye and its application in dye-sensitized solar cells. *Plasma Sci. Technol.* **2006**, *8* (5), 531.
(38) Andersson, G.; Morgner, H.; Pohl, H. Energy-loss straggling of helium projectiles at low kinetic energies: Deconvolution of concentration depth profiles of inorganic salt solutes in aqueous solutions. *Phys. Rev. A* **2008**, *78* (3), 032904.
(39) Andersson, G.; Krebs, T.; Morgner, H. Activity of surface active substances determined from their surface excess. *Phys. Chem. Chem. Phys.* **2005**, *7* (1), 136−142.
(40) Nazeeruddin, M. K.; De Angelis, F.; Fantacci, S.; Selloni, A.; Viscardi, G.; Liska, P.; Ito, S.; Takeru, B.; Grätzel, M. Combined Experimental and DFT-TDDFT Computational Study of Photoelectrochemical Cell Ruthenium Sensitizers. *J. Am. Chem. Soc.* **2005**, *127* (48), 16835−16847.
(41) Shklover, V.; Nazeeruddin, M. K.; Zakeeruddin, S. M.; Barbé, C.; Kay, A.; Haibach, T.; Steurer, W.; Hermann, R.; Nissen, H. U.; Grätzel, M. Structure of Nanocrystalline TiO2 Powders and Precursor to Their Highly Efficient Photosensitizer. *Chem. Mater.* **1997**, *9* (2), 430−439.
(42) Atkins, P. *Physical Chemistry*, 8th ed.; Oxford University Press: Oxford, 2006.
(43) Quinton, J.; Thomsen, L.; Dastoor, P. Adsorption of organosilanes on iron and aluminium oxide surfaces. *Surf. Interface Anal.* **1997**, *25* (12), 931−936.
(44) Quinton, J. S.; Dastoor, P. C. The effect of experimental conditions on the oscillatory adsorption of propyltrimethoxysilane on aluminium oxide surfaces. *Appl. Surf. Sci.* **1999**, *152* (3−4), 131−137.
(45) Feldt, S. M.; Gibson, E. A.; Gabrielsson, E.; Sun, L.; Boschloo, G.; Hagfeldt, A. Design of Organic Dyes and Cobalt Polypyridine Redox Mediators for High-Efficiency Dye-Sensitized Solar Cells. *J. Am. Chem. Soc.* **2010**, *132* (46), 16714−16724.
(46) Lee, K. E.; Gomez, M. A.; Regier, T.; Hu, Y.; Demopoulos, G. P. Further Understanding of the Electronic Interactions between N719 Sensitizer and Anatase TiO2 Films: A Combined X-ray Absorption and X-ray Photoelectron Spectroscopic Study. *J. Phys. Chem. C* **2011**, *115* (13), 5692−5707.
(47) Dürr, M.; Schmid, A.; Obermaier, M.; Yasuda, A.; Nelles, G. Diffusion Properties of Dye Molecules in Nanoporous TiO2 Networks. *J. Phys. Chem. A* **2005**, *109* (17), 3967−3970.
(48) Franco, G.; Peter, L. M.; Ponomarev, E. A. Detection of inhomogeneous dye distribution in dye sensitised nanocrystalline solar cells by intensity modulated photocurrent spectroscopy (IMPS). *Electrochem. Commun.* **1999**, *1* (2), 61−64.